Potential Distribution in a Fluidized Bed Electrode

Tülay ESKİKAYA
Chemistry Department, Istanbul Technical University, Maslak 80626, Istanbul, Turkey
(Received January 23, 1989)

A study is described on the measurements of potential distribution in the bed and electrolyte of a hydrogen peroxide depolarized fluidized bed electrode consisting of 10 grams of silver coated glass beads in a cell of cyclindrical geometry. The results of potential profiles show that the electrode potentials both in static and fluidized beds were uniform throughout most of the bed. In the latter case, however, the degree of deactivation in the top of the bed is less than for a static bed, which explains current from fluidized bed. The variation of the charge-transfer coefficient along the bed, which is of great importance from the point of the performance of a fluidized bed electrode, is also determined.

In order to understand the functioning of a fluidized bed electrode, the potential distribution in the bed and electrolyte is of great importance. Some work has been done on this line before.[1-8] A direct measurement of electrode potentials was suggested by Backhurst,[1] by means of a pseudo-particle. Hiddleston and Douglas[2,3] recorded bead potentials with respect to the feeder by using a similar probe to that suggested by Backhurst. Mason,[4,5] on the other hand, recorded the frequency of the collisions on the free beads with the pseudo-bead per unit time and the variation in probe potentials as a result of the collisions. A mathematical model for the charge transfer in fluidized bed electrodes was developed by Goodridge et al.[6] Huh[7] also measured the particle and electrolyte potentials and overvoltages in fluidized bed electrodes of two different types. Rojo et al.[8] developed a capacitor model to determine the electric change in fluidized beds on the basis of voltage measurements between a probe and a metallic distributor. Many new contributions by the others, however, are still continuing on the same subject.

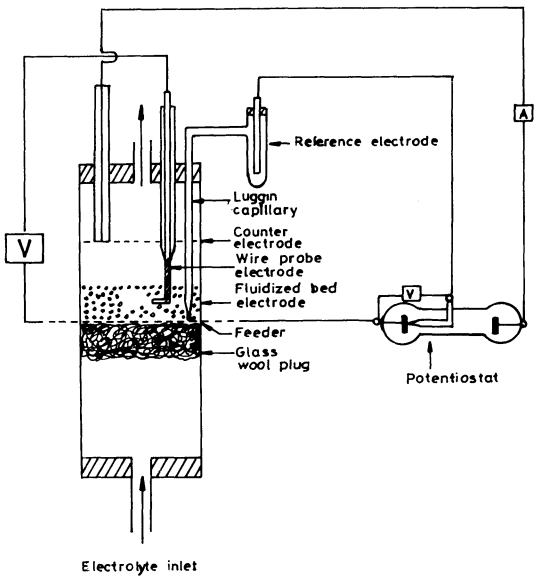

Fig. 1. Experimental cell and potentiostat.

Experimental

Fluidized Bed Material and Catalyst. Potential distribution measurements in the solution and in the bed were studied for a hydrogen peroxide depolarized fluidized bed electrode. The concentrations of the reactant and the electrolyte used during the measurements were 4.1×10^{-2} mol dm^{-3} hydrogen peroxide and 5.0 mol dm^{-3} KOH, respectively.

The body of fluidized beds consisted of "Ballotini" glass beads (mean diameter 600 μm, diameter range 520—690 μm) coated with silver from a solution containing it in the form of ammonia complex and to reduce ammonia complex glucose was used.[9,10] The silver layer acted as both a conducting surface and catalyst. The final mean density of the beads 3.0 g cm^{-3} and the geometric area 33 cm^2 g^{-1}.

Apparatus. The experimental cell system which was used with a potentiostat power supply is shown in Fig. 1. It consisted of two lengths of 2.54 cm dia., Perspex tube joined with an expanded silver coated nickel mesh (strand size 0.00127×0.00127 cm; 772 appertures per cm; mesh 9.8 LWM ×17.7 SWM per cm; free area 60%) stretched between the two sections. A glass wool plug beneath the mesh smoothed the electrolyte flow through the bed. The mesh acted as bed support and electrical contactor to the beads. A nickel mesh counter electrode was situated above the bed. A mercury-mercurly(II) oxide reference electrode was connected to a Luggin capillary, the tip of which was adjacent to the feeder, thus, the feeder potential was controlled.

Other equipments used included an Amel potentiostat capable of giving 10 A at 50 V and a Solartron high impedance voltmeter having a voltage input ranging from ±0.1995 V to 1995 V for measurements of the bed and solution potentials with secondary probes. A Pye cathetometer (accuracy ±0.005 mm) was used to measure bed heights.

Solutions were made up from Analar grade reagents using once-distilled water.

Experimental Procedure. The weight of the bed was 10 g, giving a mean static bed height of 1.16 cm. Fluidizations are quoted as a percentage increase in bed height over the static bed height.

(a) Potential Distribution in the Electrolyte. Potential distribution in the solution within the bed was measured by means of a Luggin capillary which was connected to a mercury-mercury(II) oxide reference electrode. The Luggin capillary was traversed up and down through the bed and at various Luggin capillary positions, solution potentials, ϕ_s,

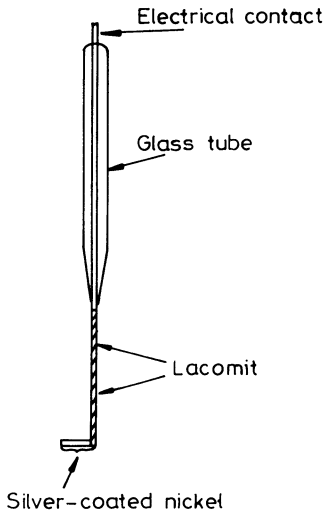

Fig. 2. Wire probe design.

were measured against the feeder.

(b) Potential Distribution in the Bed. For the potential distribution measurements in the bed two different types of probes namely, bead and wire probes were used. The bead probes were prepared by attaching a bead of bed material (600 μm dia. silver plated glass bead) to a nickel wire (0.39 mm dia.) by means of a silver impregnated epoxy resin adhesive (J.M.C. Thermosetting silver cement FSP 49). The wire was insulated from the bed by coating with "Lacomit" varnish. This type of probe was found to be unsatisfactory. A simpler method was adopted, therefore, in which a nickel wire was sealed into a glass road leaving the top end free as electrical contact and the other end of this wire probe, which was bended through 90° providing a horizontal section, acted as pseudo-bead[1,4] (Fig. 2). This pseudo-bead could be made of any area by coating the wire with Lacomit and leaving the correct amount of bare wire projecting. Any oxide film on nickel wire probe was removed by immersing it in dilute hydrochloric acid and then nickel wire was coated with silver in the same way as the plating of the beads. By coupling a Solatron high-impedance voltmeter between the probe and the feeder, it is possible to measure the bead potentials, ϕ_m, which are the potentials detected by the pseudo-bead probe electrode against the feeder electrode.

In order to find the optimum area of the pseudo-bead which would provide the actual potential of beads, potential distribution measurements in the bed were recorded with four different size of wire probes, namely "tip, small, medium and large" having surface areas of silver activated part of 0.477 mm², 1.528 mm², 3.820 mm², and 12.990 mm², respectively.

Results

In Fig. 3 distribution of the solution potential was plotted against x/l, where x is the probe position in the bed relative to the feeder and l is the bed height for 15.0—15.9% fluidized bed at three different applied potentials. As can be seen from the figure the reaction at the feeder surface is insignificant, $\frac{d\phi_s}{dx}=0$ at $x=0$,

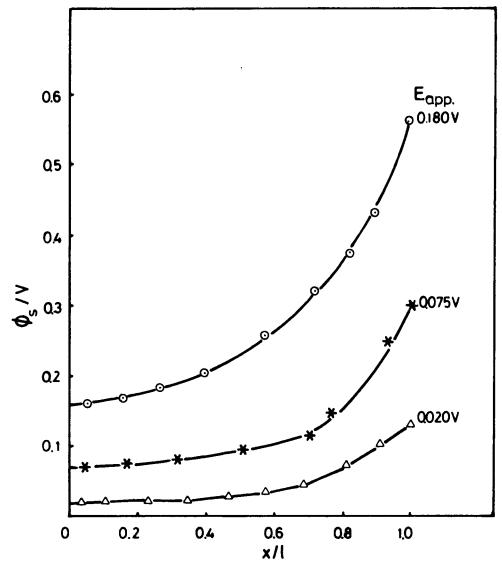

Fig. 3. Potential distribution in solution for a 15% fluidized bed at three different applied potentials.

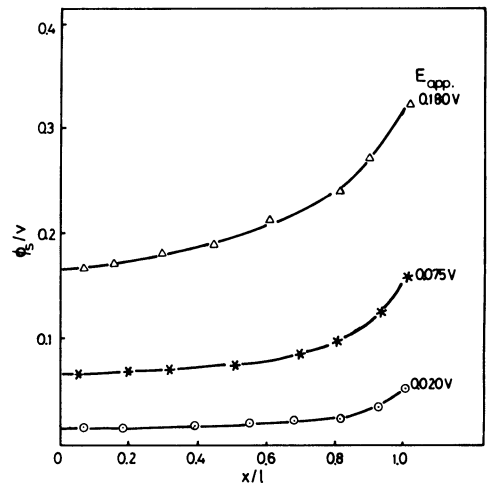

Fig. 4. Potential distribution in solution for the static bed at three different applied potentials.

(where ϕ_s is the solution potential and $x=0$ corresponds to the base of the bed) which satisfies the boundary condition of the following equation developed by Goodridge et al.[6]

$$-\frac{d}{dx}\left(K_s\frac{d\phi_s}{dx}\right)=A_pF(\phi) \quad (1)$$

where A_p is the superficial geometric area of the beads per unit volume of bed in the fluidized state, K_s is the effective specific conductance of the electrolyte in the fluidized bed and $F(\phi)$ is the dependency of current density on, ϕ, electrode potential which is the potential throughout the bed against the feeder.

Figure 4 shows the potential distribution in the solution for the static bed.

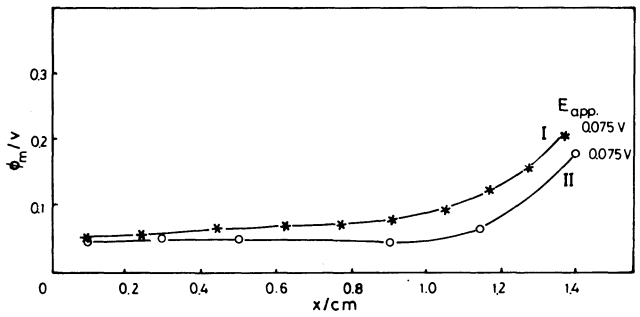

Fig. 5. Potential distribution in a 15% fluidized bed at an applied potential of 0.075 V, large (I) and tip (II) probes.

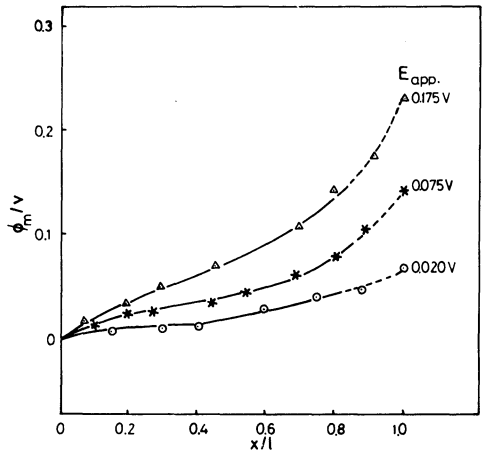

Fig. 6. Potential distribution in a 15% fluidized bed at three different applied potentials, small wire probe.

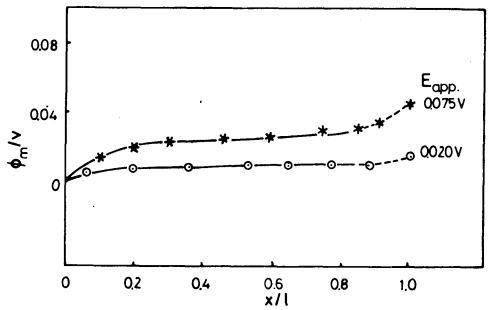

Fig. 7. Potential distribution in the static bed at two different applied potentials, small wire probe.

The potential distribution measurements in the bed taken only with the small and medium probes were quite the same. Figure 5 shows the results for large probes (Curve I) and tip probes (Curve II) for a 15% fluidized bed.

Results of the potential measurements in the bed with four different size of wire probes have shown that the surface area of an adequate probe should not be less than that of the beads, but it should be larger to some extent (the maximum and minimum surface area of the bead used in the experiments were 1.50 mm^2 and 0.85 mm^2 and the active surface area of the small and medium probes were 1.528 mm^2 and 3.82 mm^2, respectively). Since the surface area of the small probe was nearly the same as the beads and the reproducibility of the results recorded with this probe was better than a bead probe, the small probe was used throughout the potential distribution measurements in the bed.

The results recorded by the large probe can be explained by the great influence of the solution on the probe. This probe had an active area of 12.99 mm^2 and the length of the activated part of the probe was 1.35 cm which was more than the half diameter of the bed. There was not enough bead collisions with the probe and its potential was greatly governed by the potential of the solution.

With the tip probes, however, there was a few bed contact with the probe and it was nearly at its rest potential. The deviations observed at the top of the bed was again due to the effect of solution on the probes.

Figure 6 shows the potential distribution of the fluidized beds at three different applied potentials (E_{app}=0.020 V, 0.075 V, and 0.175 V). The dotted line in the figure shows the deviation of the potential at the top of the bed due to the effect of the solution potential on the probe. This could be explained by the assumption that there was not sufficient bead contact on the probe and also 3—4 rows of the beads at the top of the bed were probably not in good contact with the rest of the bed. Comparing the slope of this part of the curve with that of corresponding solution potential curve suggests a 60% solution potential effect on the probe measurement.

Figure 7 shows the potential distribution in the static bed. As can be seen from the figure, after a drop in the potential near to the feeder, the potential distribution in the static bed appeared almost constant through the bed except the slight deviation at the top.

In the operation of a fluidized bed electrode the variation of charge-transfer coefficient (K_m) along the bed has great importance on its performance. In order to observe the general tendency of the variation of charge-transfer coefficient in the fluidized bed, the values of K_m at various points of the bed were calculated using the following equations.[6]

$$I_s = -K_s A\left(\frac{d\phi_s}{dx}\right) \tag{2}$$

$$I_m = -K_m A\left(\frac{d\phi_m}{dx}\right) \tag{3}$$

where I_s is the current flow through the electrolyte, ϕ_s is the solution potential, I_m is the current flow in the bed and A is the area of current flow perpendicular to the direction of flow which is equivalent to the area of the feeder, i.e. 5.06 cm^2.

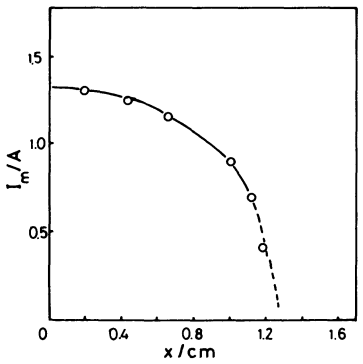

Fig. 8. Variation of current flow along 15% fluidized bed at an applied potential of 0.075 V.

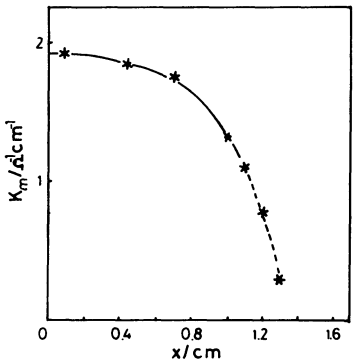

Fig. 9. Variation of charge-transfer coefficient along 15% fluidized bed at an applied potential of 0.075 V.

The current flow through the electrolyte, I_s, was calculated through Eq. 2. The values of $\frac{d\phi_s}{dx}$ were determined from the point slopes of Fig. 3. The effective conductivity of the electrolyte, K_s, which was determined from the Bruggeman relationship, quoted by Goodridge[6] as

$$K_s = \rho \cdot \varepsilon^{3/2} \quad (4)$$

where ε is the bed voidage and ρ is the specific conductivity of the electrolyte. ρ is taken as 0.53 ohm^{-1} cm^{-1} for 5.0 mol dm^{-3} KOH.[11] This equation provides the value of K_s as 0.2247 ohm^{-1} cm^{-1}.

The values of I_s were substracted from the total current values and the values of the current flow in the bed, I_m, were obtained for various points of the bed. The current flow in the bed ceases at the bed boundary so all the current is supported by the solution and at the top of the bed the current flow through the electrolyte should be equal to the total current of the bed. Figure 8 shows the results for a 15% fluidized bed at an applied potential of 0.075 V.

Similary $\frac{d\phi_m}{dx}$ values at various points of the bed can be found from the potential distribution in the bed and since the values of I_m are known, K_m can be obtained from Eq. 3.

Figure 9 shows the variation of charge-transfer coefficient along the bed. The tendency of the curve corresponding to the top of the bed was again represented with a dotted line because of the possibility of the incorrect values of I_m and K_m due to the deviation in the ϕ_m vs. x curve in this region of the bed.

In Fig. 10 the electrode potentials, ϕ, which is $\phi_m - \phi_s$, of a 15% fluidized bed was plotted against x/l at a feeder potential of 0.075 V. From the figure it is shown that the electrode potential is uniform throughout the bed except at the top.

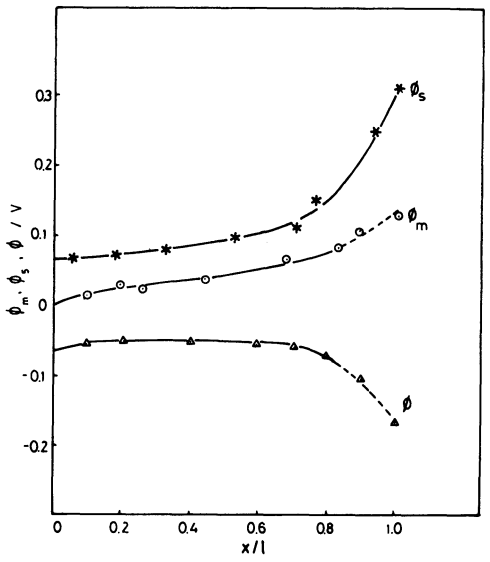

Fig. 10. Potential profiles in a 15% fluidized bed at an applied potential of 0.075 V, electrolyte, ϕ_s; beads, ϕ_m; and electrode potential, ϕ.

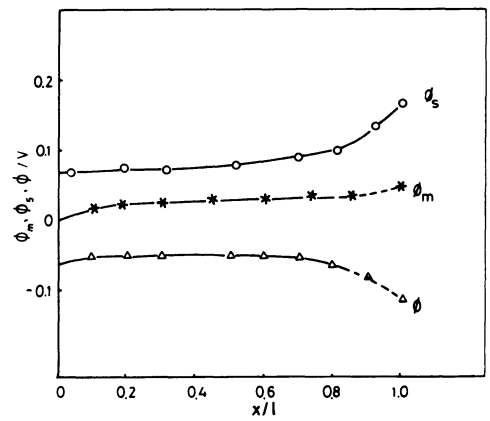

Fig. 11. Potential profiles in the static bed at an applied potential of 0.075 V, electrolyte, ϕ_s; beads, ϕ_m; and electrode potential, ϕ.

Figure 11 shows the electrode potential for the static bed at the feeder potential of 0.075 V.

Discussion

In porous and similar electrodes the physical properties of the electrode material and its porosity may determine the conductivity of electrode. In a fluidized bed electrode, however, the conductivity is not only a function of bed material. For fluidized beds, Goodridge et al.[6] have introduced the concept of the charge-transfer coefficient, K_m, which is not only dependent on the physical properties of bed material but also electrode reaction and hydrodynamic conditions in the bed. The value of K_m and its variation in the bed are of great importance from the point of the performance of a fluidized bed electrode.

The measurements of potential distribution in the bed and electrolyte showed that the electrode potentials both in a static and 15% fluidized beds were uniform throughout most of the bed except at a region corresponding to the top of the bed (Figs. 10 and 11). In the uniform distribution of potential electrode reactions occuring at low current densities, the comparable values of the charge-transfer coefficient and the effective specific conductance of the electrolyte which were 0.2247 $ohm^{-1} cm^{-1}$ and 0.53 $ohm^{-1} cm^{-1}$, respectively, in the present work, might be the important factor.

In comparison of Figs. 10 and 11 shows that the deviation of the fluidized bed curve from the static bed curve seems to indicate that there is more current supported at the top of the bed by the fluidized bed than the static bed.

References

1) J. R. Backhurst, Ph. D. Thesis, Univ. Newcastle (1967).

2) J. N. Hiddleston and A. F. Douglas, *Nature (London)*, **218**, 601 (1968).

3) J. N. Hiddleston and A. F. Douglas, *Electrochim. Acta*, **15**, 431 (1970).

4) R. Mason, Ph. D. Thesis, Univ. Newcastle (1969).

5) T. Berent, R. Mason, and I. Fells, *J. Appl. Chem. Biotechnol.*, **21**, 71 (1971).

6) F. Goodridge, I. Holden, H. D. Murray, and R. E. Plimley, *Trans. Inst. Chem. Eng.*, **491**, 128 (1971).

7) T. Huh, Energy Res. Abstr. 10, Abstr. No. 34287 (1985).

8) V. Rojo, J. Quardiola, and A. Vian, *Chem. Eng. Sci.*, **41**, 2171 (1986).

9) G. A. Dalin, "Encyclopedia of Chemical Technology," Interscience, New York (1954), Vol. 12, p. 443.

10) C. J. Smithells, "Metal Reference Book," Butterworths, London (1967), Vol. 3, p. 1100.

11) J. O'M. Bockris and S. Srinivasan, "Fuel Cells: Their Electrochemistry," McGraw-Hill Book Co., New York (1969).